Title

Oxytocin is an age-specific circulating hormone that is necessary for muscle maintenance and regeneration.

Journal

Nature communications, 5(1)

ISSN

2041-1723

Authors

Elabd, Christian
Cousin, Wendy
Upadhyayula, Pavan
et al.

Publication Date

2014-06-01

DOI

10.1038/ncomms5082

Peer reviewed

HHS Public Access

Author manuscript

Nat Commun. Author manuscript; available in PMC 2015 July 23.

Published in final edited form as:

Nat Commun. ; 5: 4082. doi:10.1038/ncomms5082.

Oxytocin is an age-specific circulating hormone that is necessary for muscle maintenance and regeneration

Christian Elabd[#], **Wendy Cousin**[#1], **Pavan Upadhyayula**, **Robert Y. Chen**, **Marc S. Chooljian**, **Ju Li**, **Sunny Kung**, **Kevin P. Jiang**, and **Irina M. Conboy**[1]

Department of Bioengineering, Stem Cell Center, and QB3 Institute, UC Berkeley, Berkeley, CA 94720, USA; University of California, Berkeley B107B Stanley Hall #1762 Berkeley, CA 94720-1762

[#] These authors contributed equally to this work.

Abstract

The regenerative capacity of skeletal muscle declines with age. Previous studies suggest that this process can be reversed by exposure to young circulation, but systemic age-specific factors responsible for this phenomenon are largely unknown. Here we report that oxytocin- a hormone best known for its role in lactation, parturition, and social behaviors - is required for proper muscle tissue regeneration and homeostasis, and that plasma levels of oxytocin decline with age. Inhibition of oxytocin signaling in young animals reduces muscle regeneration, whereas systemic administration of oxytocin rapidly improves muscle regeneration by enhancing aged muscle stem cell activation/proliferation throughactivation of the MAPK/ERK signalling pathway. We further show that the genetic lack of *oxytocin* does not cause a developmental defect in muscle, but instead leads to premature sarcopenia. Considering that oxytocin is an FDA approved drug, this work reveals a potential novel and safe way to combat or prevent skeletal muscle aging.

INTRODUCTION

The proportion of people over the age of 60 is growing faster than any other age group, as a result of both longer life expectancy and declining fertility rates, thus enhancing the quality of life as age of people is of major importance. With aging, the capacity of our tissues to maintain homeostasis and regenerate declines and eventually fails, leading to degenerative disorders and eventual organ failure. The reduction in muscle mass in humans starts in the

[1]**Corresponding authors:** Irina M. Conboy: iconboy@berkeley.edu; (+1) 510 666 2792; Wendy Cousin: wendy.cousin@gmail.com; (+1) 510 224 4422.

AUTHOR CONTRIBUTIONS

CE and WC designed, planned, performed, analyzed and interpreted the experiments for Figures 1, 2, 3, 4, 5d-f, 6, 7, and Supplementary Figure 1, and wrote the manuscript. RYC, MSC, and SK, performed experiments and contributed to data analysis for Figures 2b, 4, and 6a. KPJ performed experiments and contributed to data analysis for Figure 3c, 6e-g and Supplementary Figure 1. PU performed experiments and contributed to data analysis for Figures 2d, 3c, 5d-e, 6c-d, 7c-d. JL designed, planed, performed, analyzed and interpreted the experiments for Figure 5a-c and Supplementary Figure 2. IC designed, guided and integrated the work, interpreted the data, and wrote the manuscript.

COMPETING FINANCIAL INTERESTS

The authors have no conflict of competing interest to declare.

third decade of life and accelerates after the fifth decade, resulting in a decrease in strength and agility[1]. Muscle aging is characterized by a deficiency in muscle regeneration after injury and by muscle atrophy associated with altered muscle function, defined as sarcopenia[2]. The limiting step in muscle regeneration after injury is the activation of the muscle stem cells, or satellite cells. They need to break quiescence and proliferate in order to form new myofibers or fuse with damaged ones. Satellite cells from old muscle are intrinsically able to repair damaged muscle, but are reversibly inhibited by the aged niche, yet can be quickly rescued for productive tissue repair by a number of experimental methods, including heterochronic parabiosis[3]. While the rejuvenating effects of heterochronic parabiosis have been observed in several tissues such as muscle, brain, liver, pancreas, and heart[4-9] the molecular mechanisms are not fully understood and only a few potential systemic factors responsible for this phenomena have been identified. A few pro-aging circulating factors which increase in old animals have been identified, including TGF-β and Wnt signaling pathway effectors, which are deleterious for muscle regeneration[5,10], as well as the CCL11 chemokine that leads to impaired neurogenesis and decreased cognition and memory[6]. To date, few circulating molecules decreasing with age have been identified to be responsible for skeletal muscle aging

Considering that oxytocin (OT) levels decrease after ovariectomy, which mimics hormonal aging[11] and that myoblasts express the oxytocin receptor (OTR)[12], we hypothesized that OT might be among the key circulating age-specific determinants of maintenance and repair of skeletal muscle. OT is a nonapeptide mainly produced by the hypothalamus and stored in the neurohypophysis. It acts via its receptor both centrally as a neuromodulator and peripherally as a hormone, released by the neurohypophysis into the circulation. The OTR is a class I G-protein-coupled receptor, which upon OT binding activates protein kinase C and induces intracellular calcium release that acts as a second messenger to induce a cascade of intracellular changes and activity[13]. OT is best known for its role in lactation and parturition[14] as well as in social behaviors, promoting trust and bonding[15]. While the role of OT in supporting tissue homeostasis and regeneration is poorly documented, recent published work proposed a role of OT in preventing osteoporosis and obesity[11,16-20] and in improving myocardium recovery after ischemic injury[21]. Additionally, OT has been shown to facilitate *in vitro* differentiation of mesenchymal stem cells toward cardiomyogenesis and osteogenesis and to inhibit adipocyte differentiation[11,22].

Here we show that plasma levels of oxytocin and the levels of oxytocin receptor in muscle stem cells dramatically decline with age and demonstrate that oxytocin is required for skeletal muscle tissue regeneration and homeostatic maintenance. Importantly, we show that short-term systemic OT delivery restores muscle regeneration in old mice by improving aged muscle stem cell function, while pharmacologic attenuation of OT signaling with a selective antagonist alters muscle regeneration in young mice. Confirming the dependence of muscle maintenance and repair on oxytocin, mice deficient for *Ot* present signs of premature muscle tissue aging: defective muscle regeneration and a decrease in muscle mass and fiber size characteristic of sarcopenia at only 12 months of age. Our results suggest that OT per se or deliberate modulation of OT signaling could become a potential treatment to combat the age-related decline in muscle tissue maintenance and repair.

RESULTS

Systemic OT and OTR levels in satellite cells decline with age

Since circulating OT levels decrease after ovariectomy, which mimics hormonal aging[11], we hypothesized that its level would decrease during natural aging. OT plasma levels were measured in young (2-4 month old) and old (18-24 month old) C57/BL6 male mice, using an OT-specific enzyme immunoassay. A significant 3-fold decrease was observed in aged mice as compared to young, suggesting that endocrine levels of OT decline with age (Fig. 1a). Little is known about the expression of the oxytocin receptor (OTR) in skeletal muscle either in general or in an age-specific way; thus we examined OTR protein expression in young and old skeletal muscle. Western blotting analysis demonstrates that OTR is detected in whole skeletal muscle (Fig 1b). Similar levels of OTR were observed in young and old whole muscle lysates that contain, in addition to proteins from muscle fibers and satellite cells, proteins from other cell types including vascular and immune cells, adipocytes and fibroblasts (Fig. 1b, d). Notably, when protein lysates were prepared from muscle stem cells, OTR was found to be expressed at significantly higher levels in young satellite cells as compared to old (Fig. 1c, e). These results demonstrate that with aging the decline in the circulating OT hormone is compounded by diminished levels of OTR in the old muscle stem cells. Confirming the western blotting data, immunofluorescence analysis of muscle tissue sections revealed that OTR was indeed expressed in cells that were observed in the satellite cell position (Fig. 1f, top) and co-localized with the satellite cell marker Pax7 in quiescent and injury-activated satellite cells (Fig. 1f, middle panels). Although most Pax7-positive satellite cells express OTR, expression of this receptor was also observed in many Pax7-negative cells (Fig. 1f), suggesting that OT acts on several cell types in skeletal muscle.

Systemic decline in OT causes poor regeneration of old muscle

To determine whether the age-specific decrease in systemic OT is responsible for the decline in muscle regeneration that is typical of old mice, we systemically administered OT to old mice and an OT-selective antagonist (OTA) to young mice and studied the success in muscle regeneration after cardiotoxin-induced injury. The schematic for this study is shown in Figure 2a. Five days post injury, robust muscle regeneration was observed in young mice, based on the high numbers of newly-formed (eMyHC+) fibers with centrally-located nuclei in the injured area (Fig. 2b, c). As expected, a significant decline in the formation of new muscle fibers was evident in old mice. Interestingly, subcutaneous injections of OT improved muscle regeneration in the old mice to a level comparable to the young. In young mice, in which muscle regeneration occurs efficiently, ectopic OT had no effect (Fig. 2b, c). Importantly, a significant decrease in muscle regeneration, to a level similar to that seen in old mice, ensued when young mice were administered with OTA (Fig. 2b, c).

The deficiency in skeletal muscle regeneration observed in aged mice is associated with an increase in fibrotic tissue formation[5,23]. As expected, the fibrotic index was greater in old mice as compared with young (Fig. 2d and Supplementary Fig. 1a). Ectopic OT significantly decreased the fibrotic index in old mice, whereas OTA injections increased fibrosis in young mice (Fig. 2d and Supplementary Fig. 1a).

These data demonstrate that one consequence of the age-specific systemic decline in OT is poor regeneration of skeletal muscle accompanied by increased fibrosis. Importantly, ectopic OT rapidly rescued repair of damaged old muscle, while OTA quickly incapacitated the regeneration of young muscle.

OT mediates the regenerative potential of muscle stem cells

Satellite cell activation/proliferation are the main limiting steps in old muscle regeneration. Exposure to a young environment has been shown to restore muscle regeneration by promoting satellite cell proliferation[3,4,24]. Since ectopic OT exposure over a short period of time rescued the repair of damaged old muscle, we evaluated whether the decreased level of OT in old was responsible for the lack of satellite cell proliferation *in vivo*. OT was administered to old mice daily starting 6 days prior to cardiotoxin-induced muscle injury (Fig. 3a). To monitor cell division *in vivo*, BrdU was injected subcutaneously 12 hours prior to euthanasia. Three days after injury, tibialis anterior muscles were isolated, and the percentages of BrdU and Desmin double positive cells (i.e. proliferating myogenic progenitor cells that were generated by satellite cells activated in response to tissue injury) were quantified in the injury area in muscle sections (Fig. 3b, c). As we have previously published, these myogenic cells co-express Pax7 and Desmin, while the non-myogenic Desmin-positive cells represent less than 2% in such experiments[25,26]. A 3-fold decrease in myogenic cell proliferation was observed in old muscles as compared with young (Fig. 3c). Importantly and in agreement with the rescue of muscle repair, ectopic OT significantly improved myogenic cell proliferation *in vivo* (Fig. 3c).

To further study the effect of OT on satellite cell proliferation and differentiation, we performed an *ex vivo* analysis, as described in the schematic of Figure 4a. Three days post injury, muscles were isolated and digested into bulk myofibers as previously described[4,24,25,27] and cells were cultured in their own mouse's respective serum for 24 hours (Fig. 4a). In order to label the cells that were activated *in vivo* in response to muscle injury, BrdU was injected subcutaneously 12 hours prior to euthanasia. Myogenic proliferation of cells activated *in vivo* was quantified by calculating the percentage of BrdU and Desmin double positive cells, which as mentioned above is a sensitive and accurate way to measure the age-specific differences in myogenicity[24,25,27]. A 41% decrease in proliferation was observed in the old activated satellite cells as compared with young (Fig. 4b, c). Confirming the *in vivo* data observed in Figure 3c, ectopic OT restored the myogenic proliferation of old satellite cells to a level comparable to young. Moreover, decreased myogenic proliferation was observed when young mice were treated with OTA (Fig. 4b, c). We also observed that the proliferation of activated satellite cells derived from young mice administered with OT tended to increase.

To study whether these Brdu and Desmin double-positive satellite cell progeny were functionally competent, we evaluated their myogenic differentiation potential. As illustrated in Figure 4a, cells isolated from muscles at 3 days post injury were cultured for 24 hours in their mouse's respective serum and were switched to differentiation medium for 48 hours, when a pronounced age-specific decline in generation of de-novo myotubes is typically detected. The myogenic fusion index (the number of nuclei included in *de novo* formed

eMyHC+ myotubes as a fraction of the total nuclei), was then scored to assess cell differentiation. Supporting the observed increase in the number of newly-regenerated eMyHC+ fibers *in vivo* after OT injection (Fig. 2b, c), systemic administration of OT to old mice rejuvenated the myofiber-forming capacity of satellite cells responding to tissue injury (Fig. 4d, e). In agreement with the idea that OT is required for myogenicity, when OT signaling was antagonized in young mice not only the proliferation but also the differentiation declined to levels similar to those of old animals, with their low circulatory OT (Fig. 4d, e). These results demonstrate that myogenic proliferation and subsequent differentiation depend on "youthful" levels of OT.

Since we showed that OTR was expressed in skeletal muscle satellite cells (Fig. 1c, e and f), we hypothesized that OT acts directly on myogenic cells. To test this hypothesis, satellite cells were freshly isolated from cardiotoxin-injured muscles and plated in medium containing their own mouse serum supplemented or not with OT for 24 hours. As previously published[28] and shown in Supplementary Figure 2, satellite cell purity was similar for young and old cells and greater than 90%. OT increased the proliferative capacity of old satellite cells cultured in old serum to similar levels of young cells cultured in young serum, as shown by the increased percentage of Ki67 positive activated muscle stem cells and the diminished expression of the cyclin-dependent kinase inhibitor 1, p21 (Fig. 5a-c). No effects of OT were observed on young satellite cells, in agreement with the higher levels of endogenous OT in young circulation (Fig. 1a). OT also promoted the proliferation of primary myogenic progenitors as shown by a three-fold increase in the percentage of BrdU positive cells (Fig. 5d, e).

OT directly acts in satellite cells via the MAPK/ERK pathway

Since the MAPK signaling pathway plays an important role in muscle stem cell activation/proliferation[29-34] and phospho-ERK1/2 is a well-documented downstream effector of OT in other cell types[11,35], we postulated that OT could be a physiological inducer of MAPK, that promotes myogenic cell proliferation via the phosphorylation of ERK1/2. Indeed, addition of a MEK inhibitor (MEKi) decreased the proliferation of young satellite cells and increased the expression of p21 to old levels (Fig. 5a-c). In accordance with the idea that OT signals via MAPK in supporting adult myogenesis, the effects of ectopic OT on freshly isolated activated satellite cells and on primary myogenic progenitor cells were abolished in the presence of MEKi (Fig. 5a-e).

To confirm the ability of OT to induce ERK1/2 phosphorylation, primary myogenic progenitor cells were stimulated for 5 to 20 minutes with OT in the presence or absence of MEKi. ERK1/2 phosphorylation was greatly induced 5 minutes after stimulation with OT (Fig. 5f). At 10 minutes ERK1/2 phosphorylation started to decrease and returned to the basal level by 20 minutes (Fig. 5f). In support of functional effects of OT on myogenic cell proliferation shown above, MEKi prevented OT-induced ERK1/2 phosphorylation, reducing the levels of phospho-ERK1/2 below the basal level observed in untreated cells (Fig. 5f), all confirming activation of the MAPK pathway by its endogenous ligand for productive myogenic responses.

Ot deficient mice display premature muscle aging

To confirm these findings in a genetic model, we studied muscle regeneration after cardiotoxin-induced injury in *Ot* knockout (KO) mice (B6;129S-Oxttm1Wsy/J). As compared to their wild type (WT) littermates, we observed a progressive decline in muscle regeneration of *Ot* KO mice that was noticeable at 3 months of age and became pronounced and significant at 12 months of age (Fig. 6a, b). The decline in muscle regeneration observed between one year old WT and *Ot* KO mice is comparable to the one measured between young (2-4 month old) and old (18-24 month old) WT C57/BL6 mice. In accordance with the data on the *in vivo* decline in the myogenic cell proliferation in old C57/BL6 mice, a decrease in activated satellite cell proliferation was observed in *Ot* KO mice when compared to WT littermates (Fig. 6c). A significant decline in muscle maintenance and repair is not expected and was not observed in WT mice at 12 months of age (Fig. 6b); thus it is very interesting that the lack of OT prematurely ages the animals in this aspect.

Moreover, similarly to 24-month-old C57/BL6 old mice, 12-month-old *Ot* KO mice display prematurely increased fibrosis when compared to age-matched WT littermates (Fig. 6d, Supplementary Fig. 1b). Appearance of adipocytes within the injured area has been reported to occur after muscle injury[36-39]. The number of adipocytes within the recently regenerated or un-injured muscle (assayed by perilipin staining), was generally low and a non-significant increase was observed in *Ot* KO mice, as compared with WT animals (Fig. 6e-g). However, we observed a clear increase in perimuscular and intermuscular adipose tissue deposition around the hind limb muscles in *Ot* KO versus WT littermates (Fig. 7a), consistent with the overall adipose tissue mass increase[17].

Muscle aging is characterized by a deficiency in muscle regeneration after injury but, most importantly, by muscle atrophy and altered muscle function observed in older individuals and defined as sarcopenia[1,2]. Having demonstrated that a lack of OT resulted in the diminished regeneration of old muscle after injury we next sought to examine whether OT was involved in age-associated sarcopenia. To test this hypothesis, we assessed the mass of the gastrocnemius and the tibialis anterior muscles of 12-month-old *Ot* KO mice and their WT littermates. As shown in Figure 7b and c, *Ot* deficiency resulted in significantly smaller muscles: *Ot* KO mice displayed a 32% decrease in muscle mass for the tibialis anterior and a 22% decrease for gastrocnemius as compared to their WT littermates. We further compared the muscle histology of *Ot* KO versus WT mice by measuring muscle fiber surface area as well as the minimum Feret diameter of muscle cross section. Remarkably, there was a significant decrease in both the surface area and the minimum Feret diameter in *Ot* KO as compared to WT mice (Fig. 7d, e). Importantly, no difference was observed in the fiber surface area or in the minimum Feret diameter between WT and *Ot* KO mice when compared at 3 months of age, demonstrating that the muscle atrophy observed in *Ot* deficient mice at 12 months of age was not a consequence of a developmental defect (Fig. 7d, e). These data demonstrate that the KO in *Ot* is the first known genetic defect that results in premature sarcopenia and suggest that in the absence of OT, the non-significant but noticeable decline in muscle regeneration observed at 3 months of age might contribute to the decline in muscle fiber size and increased fibrosis and fat deposition by 12 months of age (Fig. 6b).

DISCUSSION

The role of OT in tissue homeostasis and regeneration is poorly documented and age-specific OT studies are lacking. The present work is the first to demonstrate that OT supports productive repair and maintenance of skeletal muscle, and that age-imposed decline in OT contributes to sarcopenia. Moreover, we show that OT acts directly on muscle stem cells (*in vitro* and *in vivo*) and that pro-myogenic effects of OT are mediated by MAPK/ERK signalling.

The age-specific decrease in OT receptor levels in muscle stem cells compounds the decline of OT itself, but importantly, significant OT receptor levels still remain in the old cells, allowing for an enhancement of myogenesis by ectopic OT. Interestingly, these findings are a mirror image of the age-imposed deregulation of TGF-beta/pSmad3 signaling in muscle stem cells, where with age there is an up-regulation of TGF-beta1 and simultaneous elevation of the TGF-beta receptor[24,40]. The concordant deregulation of receptors in muscle stem cells (and perhaps in tissue stem cells in general), and of the specific ligands (locally and / or in circulation) might be an interesting commonality of the aging process.

The conclusion of a pivotal role of OT in the age-specific regulation of myogenesis is emphasized by the agreement between pharmacological and genetic studies. Even though *Ot* KO mice could have developed compensations for the lack of OT and the high levels of myogenic IGF1, GH, etc. factors that are present in these animals at a young age there is already a tendency toward a decline in muscle regenerative capacity in *Ot* KO mice at 3 months of age. Such a decline is clearly manifested upon an acute administration of OT antagonist to young C57/BL6 animals. Prolong constant attenuation of muscle regeneration might contribute to premature decrease in muscle tissue health, which we observe by 1 year in *Ot* KO mice. While OT is a multifunctional hormone and future comprehensive work is needed in order to uncover its many age-specific effects on cells and tissues, this study strongly suggest that the lack of OT causes decline in myogenic responses of satellite cells, leading to an abandonment of muscle tissue maintenance.

Considering that during normal aging ubiquitin-proteasome proteolysis does not seem to cause the age-related muscle atrophy and that in contrast, muscle hypertrophy and healthy functionality cannot be sustained without effective tissue remodeling[41-43], the contribution of the age-specific decline in OT to the lack of myogenicity is a significant factor in muscle aging. Importantly, no deterioration of muscle tissue or decrease in myofiber size have been detected in the 3-month-old *Ot* KO mice, suggesting that the genetic lack of *Ot* does not cause a developmental defect, and instead specifically exacerbates sarcopenia.

To date, no effective treatment is available to treat or prevent sarcopenia and the primary recommendation remains exercise. Our work suggests that OT represents a physiological systemically present inducer of satellite cell activation/proliferation and hence, that systemic delivery of OT can counteract the defects in regeneration and maintenance of old muscle, which develop in part due to the age-specific decline in this hormone.

Our results demonstrate that OT is one of the key age-specific systemic regulators of muscle maintenance and repair; however, it is unlikely that only one circulating molecule accounts

for systemic aging or rejuvenation and other cell fate regulatory pathways have been shown to participate in these phenomena[5,24]. While other strategies such as long-term activation of the Notch signaling pathway or down-regulation of the TGF-β/pSmad and Wnt signaling pathways have been shown to be successful in acute rejuvenation of myogenesis[4,5,24] they come with side-effects such as oncogenic transformations, inadequate hematopoiesis, broad immune deregulation, etc. Therefore therapeutic modulation of key regulatory pathways is not an easy task. In contrast, OT is a naturally-produced endocrine peptide that has little to no known detrimental side effects. Diminished circulating levels of OT are associated with pathological states such as autism in children[44,45], osteoporosis[46], and depression[47]. OT is approved for use in women during parturition, has been tested to improve psychological well-being in the elderly[48], and is in clinical trials to treat autism, schizophrenia, and depression. Because of its size and structure, OT can be administered easily and by multiple routes such as by intra-nasal inhalation. The potent positive effects of OT on muscle tissue homeostasis and repair that were uncovered in this study are thus promising for developing an effective and safe new clinical strategy where OT and OTR agonists might be potentially used as systemically applicable, and sustainable molecules for combating the deterioration of muscle mass, strength, and agility in the elderly.

METHODS

Plasma preparation and oxytocin quantification

Whole blood was collected into a citrate-treated tube and spun at 700 g for 15 minutes to remove cells. Supernatant was transferred to a second citrate-treated tube, spun at 1500 g for 20 minutes to remove platelets. Plasma was aliquoted and stored at −80°c. Plasma OT concentration was measured using an Enzyme Immunoassay kit (Bachem, S-1355) according to the manufacturer's recommendation.

Animals

8-week-old male C57BL/6 mice and B6;129S-Oxttm1Wsy/J mice were purchased from the Jackson Laboratory. 22-month-old male C57BL/6 mice were purchased from the National Institute on Aging. Animals were housed and B6;129S-Oxttm1Wsy/J mice were bred at the Northwest Animal Facility (University of California, Berkeley). All procedures were performed in accordance with the administrative panel of the Office of Laboratory Animal Care, UC Berkeley. Sample size for each experiment was determined based on previously published differences between control young versus old animals in order to have sufficient statistical power, using the minimum necessary number of mice. The protocol was approved by the UC Berkeley Animal Care and Use Committee (ACUC). Mice were anesthetized by isoflurane drop and killed by cervical dislocation; blood samples were collected by heart puncture. Mice were injected daily with 50 μL of OT (1 μg g^{-1} of mice), OTA (2 μg g^{-1} of mice), or vehicle (HBSS) by interscapular subcutaneous injections.

Satellite cell preparation and cell culture

Tibialis anterior and gastrocnemius muscles of mice were injected with a total of 10 μg of cardiotoxin (Sigma-Aldrich) per leg dissolved in PBS or were left uninjured. Muscles were dissected 3 days post injury and satellite cells were derived as previously described[4,24,25].

Briefly, harvested muscles underwent enzymatic digestion in DMEM (Mediatech) containing collagenase type II (250 U mL^{-1}; Sigma-Aldrich), 10 mM HEPES, and penicillin/streptomycin antibiotics (500 IU mL^{-1}, 0.1 mg mL^{-1}; MP Biomedicals) at 37 °C for 1 hour under agitation. Fat pads and tendons were removed after a quick wash with PBS and repeated rounds of muscle trituration and sedimentation were performed to purify myofibers. Myofibers were either plated or incubated with collagenase type II (40 U mL^{-1}, Sigma-Aldrich) and dispase (2 U mL^{-1}; Invitrogen) diluted in Ham's F-10 (Mediatech), supplemented with 10% horse serum, and penicillin/streptomycin at 37 °C for 1 hour and 30 minutes under agitation. Suspensions were vortexed for 1 minute to release satellite cells from digested fibers, passed through a 40-μm cell strainer (BD Biosciences) and pre-plated on uncoated dishes for 20 minutes at 37 °C, 5% CO2. Cells that did not adhere during pre-plating were collected and plated onto Matrigel-coated (BD Biosciences) CC2-treated chamber slides (LabTek II, Thermo Fisher Scientific) in DMEM supplemented with 10% sera from the mouse they came from. Myofibers were plated in Opti-MEM (Gibco) supplemented with 10% sera from the mouse they came from for 24 hours. Myofibers were then washed away and cells were either fixed for staining or induced to differentiate in the presence of DMEM 2% horse sera for 48 hours. Primary myogenic progenitors were cultured in growth medium composed of Ham's F10 (Mediatech), penicillin/streptomycin antibiotics (500 IU mL^{-1}, 0.1 mg mL^{-1}; MP Biomedicals), and 20% Bovine Growth Serum (Life Technologies/Hyclone), supplemented with FGF-2 (6 ng mL^{-1}). To monitor the effect of OT on primary myogenic progenitor cell proliferation, cells were cultured in growth medium supplemented with OT (30 nM) alone or in combination with UO126 MEK inhibitor (10 μM). For ERK1/2 phosphorylation kinetics, primary myogenic progenitors were starved for 16 hours in Opti-MEM (Gibco) before stimulation with, OT (30 nM) alone or in combination with UO126 MEK inhibitor (10 μM) for 5, 10, 15, and 20 minutes.

Western blotting

Cells were lysed in RIPA buffer containing a protease inhibitor cocktail (Complete, Roche), PMSF, NaF, β-glycerphosphate and activated sodium orthovanadate. Whole muscle were lysed in the same buffer using a gentleMACS™ Dissociators (Miltenyi Biotec) in combination with M Tubes, to homogenize the tissue. 30 μg of total protein extract were resolved in Laemmli buffer by SDS-PAGE on pre-cast gels (Bio-Rad) and transferred to polyvinylidene fluoride (PVDF) membranes. Membranes were blocked for 30 min in 5% non-fat milk in TBS-0.05% Tween buffer. Primary antibodies against pERK1/2 (1:1000), total ERK1/2 (1:1000), pax7 (1:250), MHC (1:200), OTR (1:2000), β-Actin (1:1000) were diluted in 5% non-fat milk in TBS-0.05% Tween buffer. PVDF membranes were incubated in antibody solutions overnight at 4°C. HRP-conjugated secondary antibodies were diluted 1:4000 in 5% non-fat milk in TBS-0.05% Tween buffer and membranes were incubated for 2 hours at room temperature. Blots were subsequently developed using Amersham ECL Plus (GE Healthcare), and analyzed with a Bio-Rad Gel Doc/Chemi Doc Imaging System. Quantifications were done using Image J.

RNA isolation and Real-time RT-PCR

RNA isolation was performed using an RNAeasy Mini Kit (Qiagen) according to manufacturer's recommendations. Reverse transcription (RT) was performed using

SuperScript III First-Strand Synthesis System (Invitrogen). Real-time PCR was performed with Biorad iQ5 real-time PCR. Primers used are as follow: GAPDH-F 5′-CCACTTGAAGGGTGGAGCCA-3′; GAPDH-R 5′-TCATGGATGACCTTGGCCAG-3′; p21-F 5′-GCCCGAGAACGGTGGAACTT-3′; p21-R 5′GACAAGGCCACGTGGTCCTC-3′.

Muscle histology

We used an injury model consisting of a focal injection of cardiotoxin in the Gastrocnemius (GA) or the Tibialis anterior (TA) muscle. Muscles were dissected 3 or 5 days post injury and placed in 25% sucrose in PBS at 4 °C for 4 hours. Muscle samples were then quickly rinsed and frozen in Tissue-Tek OCT for cryosectioning. 10 μm cross-sections were stained with Hematoxylin and Eosin or Richard-Allan Scientific Gomori trichrome (Thermo Scientific) for histology analysis.

Immunocytochemistry

Cells or muscle sections were fixed for 20 minutes in 4% PFA, permeabilized with 0.25% Triton-X-100 in staining buffer (0.1% Sodium Azide and 1% Bovine Growth Serum in PBS) for 15 minutes, and incubated with primary antibody diluted in staining buffer overnight at 4 °C. Primary antibodies were diluted as following: BrdU: 1:200; Desmin: 1:200; Dystrophin: 1:200; eMyHC: 1:200; Ki67: 1:200; Myf5: 1:100; OTR: 1:100; Pax7: 1:20; Perilipin: 1:250. Cells or muscle sections were washed with staining buffer and incubated with an Alexa-Fluor conjugated secondary antibody (1:2000, Invitrogen) in staining buffer for 2 hours at room temperature, washed with staining buffer, and slides were mounted with ProLong Gold antifade reagent with DAPI (P36935, Invitrogen). An additional incubation with HCl 2.5 M for 30 minutes was performed before the permeabilization step when cells were stained for BrdU.

Chemicals and antibodies

OTA desGly-NH_2-d$(CH_2)_5$[D-Tyr^2,Thr^4]OVT is a potent OT-selective antagonist kindly provided by Pr. Maurice Manning from the University of Toledo[49,50]. OT was purchased from Bachem (H-2510). MEK inhibitor UO126 was purchased from Cell Signaling (9903) and PD98059 from Tocris (1213). Antibody against eMyHC (F1.652) and Pax7 were purchased from Developmental Studies Hybridoma Bank. Anti-OTR antibody was purchased from Proteintech (23045-1-AP). Antibody against Desmin (ab15200), Ki67 (ab15580), BrdU (ab6326) and Dystrophin (ab3149) were purchased from Abcam. Antibodies against Phospho-p44/42 MAPK (ERK1/2) (Thr202/Tyr204) and p44/42 MAPK (ERK1/2) and β-Actin were purchased from Cell Signaling (4370, 4696, and 4967 respectively). Anti-Perilipin A/B antibody was purchased from Sigma-Aldrich (P1873) and antibody against Myf5 and MHC were purchased from Santa Cruz (SC-302 and SC-20641 respectively). Fluorophore-conjugated secondary antibodies (Alexa Fluor) were purchased from Invitrogen. HRP-conjugated secondary antibodies were purchased from Santa Cruz Biotechnologies.

Fiber size

Fiber surface area and Feret minimum diameter were measure using Image J software on hematoxylin and eosin stained muscle cross sections.

Fibrosis quantification

Fibrosis was quantified as previously described [5]. Briefly, gastrocnemius muscle cross sections were immunostained for eMyHC. The total injured area and the fiber area of all eMyHC-positive fibers were measured using Image J software. The “Fibrotic Index” was calculated as: (1 − (total eMyHC+ fibers area / total injury area)) × 100%.

Supplementary Material

Refer to Web version on PubMed Central for supplementary material.

ACKNOWLEDGEMENTS

The oxytocin-selective antagonist (OTA) was kindly provided by Pr. M. Manning from Toledo University. We thank Andrea Tham and Michelle Ho for technical assistance and Eric Jabart and Michael Conboy for English proofreading of the manuscript. This work was supported by the SENS Research Foundation grant to IMC, National Institutes of Health National Institute on Aging (NIH/NIA, grant AG 027252 to IMC), California Institute for Regenerative Medecine funding (CIRM, grant RN1-00532 to IMC, CIRM postdoctoral training fellowship grants TG2-01164 to WC and CE), and Siebel Stem Cell institute training grant to WC. All authors of this paper have agreed that the two co-first authors may place either name as first when listed, because they have contributed to this work equally.

REFERENCES

1. Berger MJ, Doherty TJ. Sarcopenia: prevalence, mechanisms, and functional consequences. Interdiscip Top Gerontol. 2010; 37:94–114. [PubMed: 20703058]
2. Walston JD. Sarcopenia in older adults. Current Opinion in Rheumatology. 2012; 24:623–627. [PubMed: 22955023]
3. Conboy IM, Rando TA. Heterochronic parabiosis for the study of the effects of aging on stem cells and their niches. Cell Cycle. 2012; 11:2260–2267. [PubMed: 22617385]
4. Conboy IM, et al. Rejuvenation of aged progenitor cells by exposure to a young systemic environment. Nature. 2005; 433:760–764. [PubMed: 15716955]
5. Brack AS, et al. Increased Wnt signaling during aging alters muscle stem cell fate and increases fibrosis. Science. 2007; 317:807–810. [PubMed: 17690295]
6. Villeda SA, et al. The ageing systemic milieu negatively regulates neurogenesis and cognitive function. Nature. 2011; 477:90–94. [PubMed: 21886162]
7. Ruckh JM, et al. Rejuvenation of Regeneration in the Aging Central Nervous System. Cell Stem Cell. 2012; 10:96–103. [PubMed: 22226359]
8. Salpeter, SJ., et al. Systemic Regulation of the Age-Related Decline of Pancreatic β-Cell Replication.
9. Loffredo FS, et al. Growth differentiation factor 11 is a circulating factor that reverses age-related cardiac hypertrophy. Cell. 2013; 153:828–839. [PubMed: 23663781]
10. Carlson ME, Silva HS, Conboy IM. Aging of signal transduction pathways, and pathology. Exp Cell Res. 2008; 314:1951–1961. [PubMed: 18474281]
11. Elabd C, et al. Oxytocin controls differentiation of human mesenchymal stem cells and reverses osteoporosis. Stem Cells. 2008; 26:2399–2407. [PubMed: 18583541]
12. Breton C, et al. Presence of functional oxytocin receptors in cultured human myoblasts. J. Clin. Endocrinol. Metab. 2002; 87:1415–1418. [PubMed: 11889218]

13. Gimpl G, Fahrenholz F. The oxytocin receptor system: structure, function, and regulation. Physiol. Rev. 2001; 81:629–683. [PubMed: 11274341]
14. Soloff MS, Schroeder BT, Chakraborty J, Pearlmutter AF. Characterization of oxytocin receptors in the uterus and mammary gland. Fed. Proc. 1977; 36:1861–1866. [PubMed: 192601]
15. Lee H-J, Macbeth AH, Pagani J, Young WS. Oxytocin: The Great Facilitator of Life. Progress in Neurobiology. 2009 doi:10.1016/j.pneurobio.2009.04.001.
16. Tamma R, et al. Oxytocin is an anabolic bone hormone. Proc Natl Acad Sci USA. 2009; 106:7149–7154. [PubMed: 19369205]
17. Camerino C. Low sympathetic tone and obese phenotype in oxytocin-deficient mice. Obesity (Silver Spring). 2009; 17:980–984. [PubMed: 19247273]
18. Takayanagi Y, et al. Oxytocin receptor-deficient mice developed late-onset obesity. Neuroreport. 2008; 19:951–955. [PubMed: 18520999]
19. Deblon N, et al. Mechanisms of the anti-obesity effects of oxytocin in diet-induced obese rats. PLoS ONE. 2011; 6:e25565. [PubMed: 21980491]
20. Beranger, GE., et al. Oxytocin reverses ovariectomy-induced osteopenia and body fat gain. http://dx.doi.org/10.1210/en.2013-1688
21. Houshmand F, Faghihi M, Zahediasl S. Biphasic protective effect of oxytocin on cardiac ischemia/reperfusion injury in anaesthetized rats. Peptides. 2009; 30:2301–2308. [PubMed: 19761809]
22. Kim YS, et al. Priming of Mesenchymal Stem Cells with Oxytocin Enhances the Cardiac Repair in Ischemia/Reperfusion Injury. Cells Tissues Organs. 2011 doi:10.1159/000329234.
23. Goldspink G, Fernandes K, Williams PE, Wells DJ. Age-related changes in collagen gene expression in the muscles of mdx dystrophic and normal mice. Neuromuscul. Disord. 1994; 4:183–191. [PubMed: 7919967]
24. Carlson ME, Hsu M, Conboy IM. Imbalance between pSmad3 and Notch induces CDK inhibitors in old muscle stem cells. Nature. 2008; 454:528–532. [PubMed: 18552838]
25. Conboy IM, Conboy MJ, Smythe GM, Rando TA. Notch-mediated restoration of regenerative potential to aged muscle. Science. 2003; 302:1575–1577. [PubMed: 14645852]
26. Brack AS, Conboy IM, Conboy MJ, Shen J, Rando TA. A temporal switch from notch to Wnt signaling in muscle stem cells is necessary for normal adult myogenesis. Cell Stem Cell. 2008; 2:50–59. [PubMed: 18371421]
27. Paliwal P, Pishesha N, Wijaya D, Conboy IM. Age dependent increase in the levels of osteopontin inhibits skeletal muscle regeneration. Aging (Albany NY). 2012; 4:553–566. [PubMed: 22915705]
28. Cousin W, et al. Regenerative Capacity of Old Muscle Stem Cells Declines without Significant Accumulation of DNA Damage. PLoS ONE. 2013; 8:e63528. [PubMed: 23704914]
29. Volonte D, Liu Y, Galbiati F. The modulation of caveolin-1 expression controls satellite cell activation during muscle repair. FASEB J. 2005; 19:237–239. [PubMed: 15545301]
30. Kook S-H, et al. Cyclic mechanical stress suppresses myogenic differentiation of adult bovine satellite cells through activation of extracellular signal-regulated kinase. Mol. Cell. Biochem. 2008; 309:133–141. [PubMed: 18008139]
31. Carlson ME, et al. Molecular aging and rejuvenation of human muscle stem cells. EMBO Mol Med. 2009; 1:381–391. [PubMed: 20049743]
32. Conboy IM, Yousef H, Conboy MJ. Embryonic anti-aging niche. Aging (Albany NY). 2011; 3:555–563. [PubMed: 21666284]
33. Yousef H, et al. hESC-secreted proteins can be enriched for multiple regenerative therapies by heparin-binding. Aging (Albany NY). 2013; 5:357–372. [PubMed: 23793469]
34. Knight JD, Kothary R. The myogenic kinome: protein kinases critical to mammalian skeletal myogenesis. Skeletal Muscle. 2011; 1:29. [PubMed: 21902831]
35. Strakova Z, Copland JA, Lolait SJ, Soloff MS. ERK2 mediates oxytocin-stimulated PGE2 synthesis. Am. J. Physiol. 1998; 274:E634–41. [PubMed: 9575824]
36. Lukjanenko L, Brachat S, Pierrel E, Lach-Trifilieff E, Feige JN. Genomic profiling reveals that transient adipogenic activation is a hallmark of mouse models of skeletal muscle regeneration. PLoS ONE. 2013; 8:e71084. [PubMed: 23976982]

37. Pisani DF, Bottema CDK, Butori C, Dani C, Dechesne CA. Mouse model of skeletal muscle adiposity: a glycerol treatment approach. Biochem Biophys Res Commun. 2010; 396:767–773. [PubMed: 20457129]
38. Uezumi A, Fukada S-I, Yamamoto N, Takeda S, Tsuchida K. Mesenchymal progenitors distinct from satellite cells contribute to ectopic fat cell formation in skeletal muscle. Nat Cell Biol. 2010; 12:143–152. [PubMed: 20081842]
39. Joe AWB, et al. Muscle injury activates resident fibro/adipogenic progenitors that facilitate myogenesis. Nat Cell Biol. 2010; 12:153–163. [PubMed: 20081841]
40. Carlson ME, et al. Relative roles of TGF-beta1 and Wnt in the systemic regulation and aging of satellite cell responses. Aging Cell. 2009; 8:676–689. [PubMed: 19732043]
41. Murton AJ, Greenhaff PL. Resistance exercise and the mechanisms of muscle mass regulation in humans: Acute effects on muscle protein turnover and the gaps in our understanding of chronic resistance exercise training adaptation. Int J Biochem Cell Biol. 2013; 45:2209–2214. [PubMed: 23872221]
42. Gaugler, M., et al. PKB signaling and atrogene expression in skeletal muscle of aged mice.
43. Baehr LM, Tunzi M, Bodine SC. Muscle hypertrophy is associated with increases in proteasome activity that is independent of MuRF1 and MAFbx expression. Front. Physiol. 2014; 5:69. [PubMed: 24600408]
44. Modahl C, et al. Plasma oxytocin levels in autistic children. Biological Psychiatry. 1998; 43:270–277. [PubMed: 9513736]
45. Ruggeri B, Sarkans U, Schumann G, Persico AM. Biomarkers in autism spectrum disorder: the old and the new. Psychopharmacology. 2013:1–16. doi:10.1007/s00213-013-3290-7.
46. Breuil V, et al. Oxytocin and bone remodelling: Relationships with neuropituitary hormones, bone status and body composition. Joint Bone Spine. 2011 doi:10.1016/j.jbspin.2011.02.002.
47. Frasch A, Zetzsche T, Steiger A, Jirikowski GF. Reduction of plasma oxytocin levels in patients suffering from major depression. Adv. Exp. Med. Biol. 1995; 395:257–258. [PubMed: 8713975]
48. Barraza JA, et al. Effects of a 10-day oxytocin trial in older adults on health and well-being. Exp Clin Psychopharmacol. 2013; 21:85–92. [PubMed: 23421352]
49. Manning M, et al. Design and synthesis of highly selective in vitro and in vivo uterine receptor antagonists of oxytocin: comparisons with Atosiban. Int. J. Pept. Protein Res. 1995; 46:244–252. [PubMed: 8537178]
50. Manning M, et al. Peptide and non-peptide agonists and antagonists for the vasopressin and oxytocin V1a, V1b, V2 and OT receptors: research tools and potential therapeutic agents. 2008; 170:40.

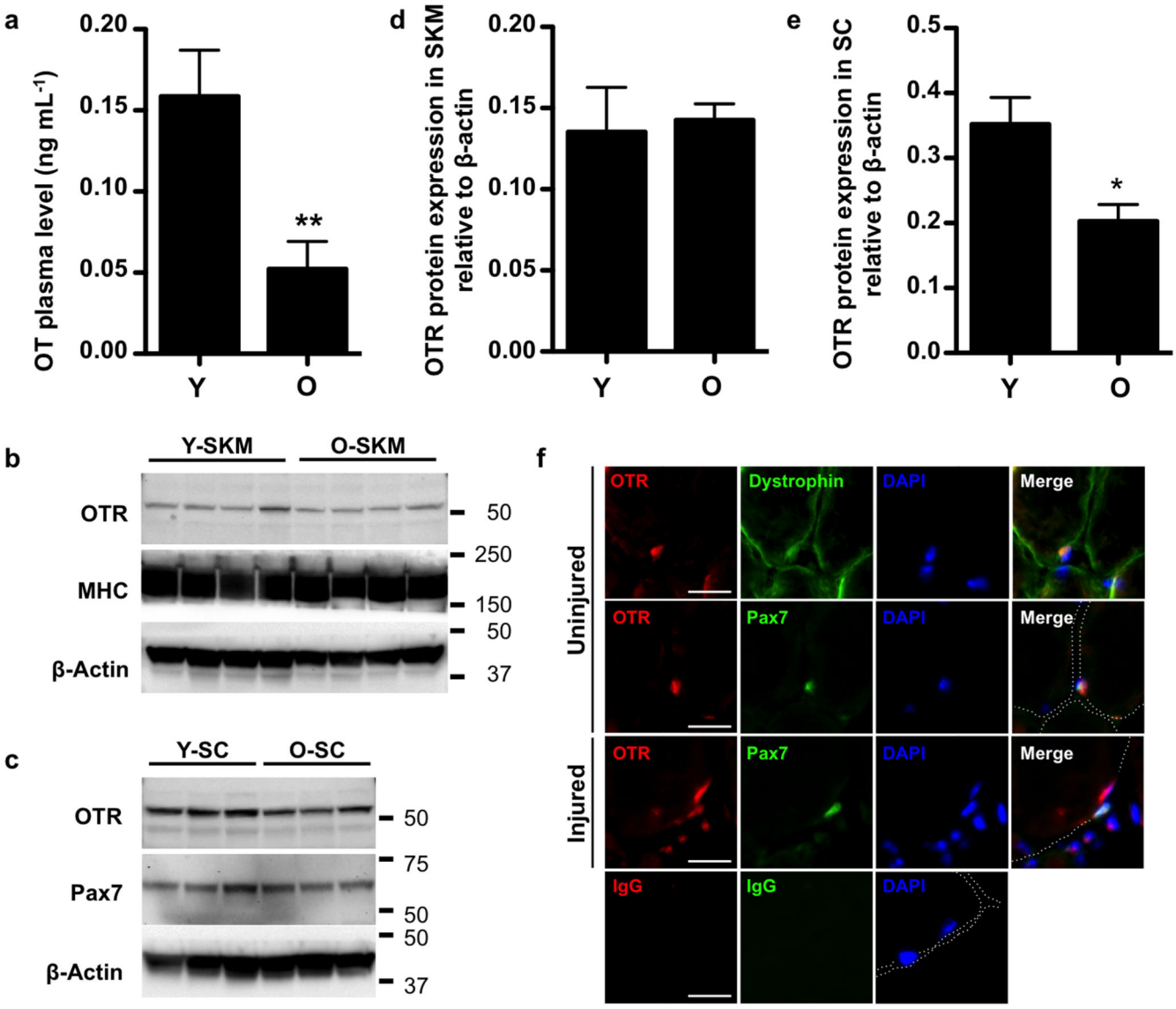

Figure 1. Systemic oxytocin declines with age and oxytocin receptor is expressed in skeletal muscle satellite cells

a, OT plasmatic levels were quantified by Enzyme Immunoassay in young (2-4 month old) and aged (18-24 month old) C57BL/6 male mice. Data represent mean ± SEM (n=6 young versus n=7 old). Two-tailed unpaired Student's t test **: *p* value < 0.01.

b and **c**, Whole skeletal muscle (GA) protein extracts (b), and hind limb satellite cell protein extracts (c) were prepared from young and old non-injured mice. Oxytocin receptor (OTR), Pax7, and myosin heavy chain (MHC) were assayed by western blot analysis. 30 μg of protein were loaded per lane and β-actin was used as a loading control. In **b** and **c**, Y-SKM: young skeletal muscle; O-SKM: old skeletal muscle; Y-SC: young satellite cell; O-SC: old satellite cell.

d and **e**, Quantification of western blot from **b**, and **c**, using Image J software. Data represent mean +/− SEM (n=4 Y-SKM, n=4 O-SKM, n=3 Y-SC, and n=3 O-SC). Two-tailed unpaired Student's t test *: *p* value < 0.05.

f, Cross sections from non-injured and 3 day-injured tibialis anterior muscle were immunostained for OTR and dystrophin or OTR and Pax7, as indicated, and counterstained with DAPI. IgG control are displayed (bottom) and dashed lines delineate muscle fibers. Scale bars represent 20 μm.

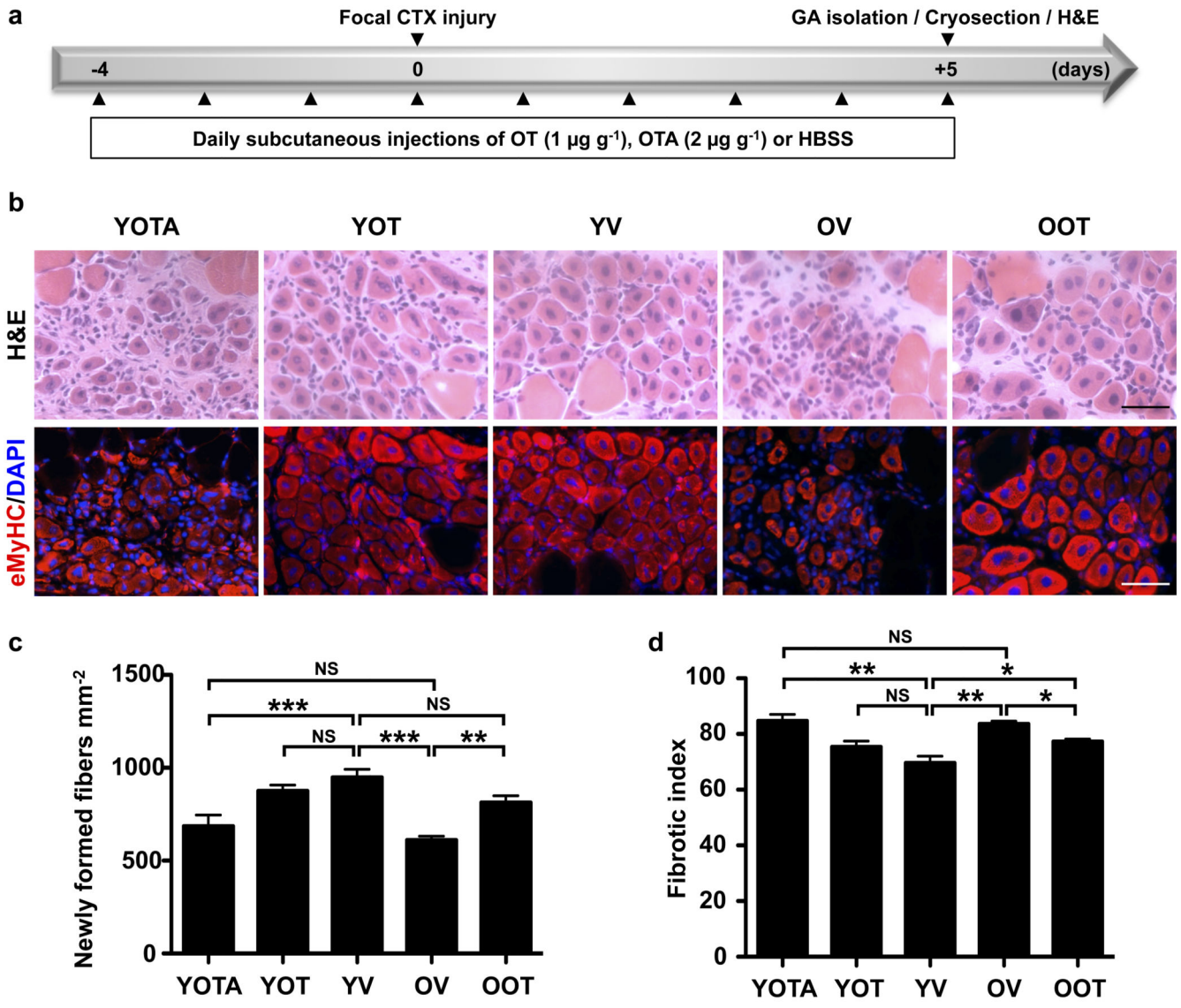

Figure 2. Age-specific systemic oxytocin decline plays a key role in the defective muscle regeneration observed upon aging

a, Schematic of the experimental procedure. Cardiotoxin (CTX) muscle injury was performed at day 0. Four days before muscle injury and over the course of the experiment, mice were administered OT (1 µg g^{-1} of mice), OTA (2 µg g^{-1} of mice), or vehicle (HBSS) daily. Five days after muscle injury, mice were killed and (GA) muscles were dissected. 10 µm cross sections were stained for hematoxylin and eosin (H&E).

b, Hematoxylin and eosin (H&E) (top) and eMyHC (bottom) staining of cardiotoxin-injured gastrocnemius muscle cross sections from mice injected with OT, OTA, or vehicle (HBSS). Scale bars represent 50 µm.

c, Muscle regeneration was quantified by scoring the number of newly-formed fibers (eMyHC positive fibers with centrally-located nuclei) in the injured area of gastrocnemius cross sections. Data represent mean ± SEM (n=9 YV, n=5 OV, n=6 YOT, n=6 OOT, n=5

YOTA). One-way ANOVA with post-hoc Newman-Keuls test **: p value < 0.01, ***: p value < 0.001, NS: Not Significant.

d, Fibrosis quantification of gastrocnemius muscle cross sections 5 days after injury. The fibrotic index represents the percentage of the injury area occupied by connective tissue. Data represent mean ± SEM (n=3 YV, n=3 OV, n=3 YOT, n=3 OOT, n=3 YOTA). One-way ANOVA with post-hoc Newman-Keuls test *: p value < 0.05, **: p value < 0.01, NS: Not Significant.

In **b-d**, YOTA: Young injected with OTA; YOT: Young injected with OT; YV: Young injected with vehicle, OV: Old injected with vehicle; OOT: Old injected with OT.

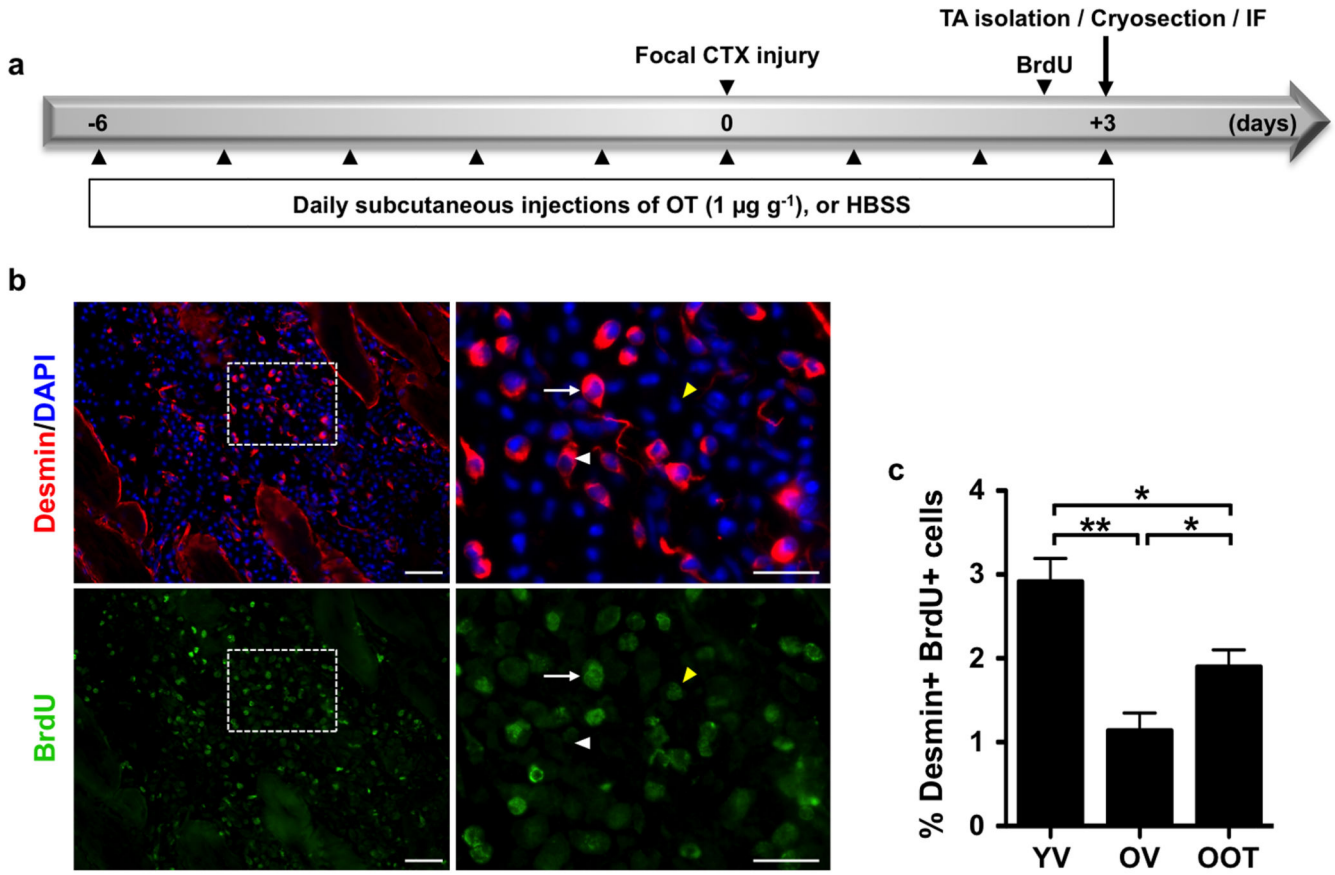

Figure 3. Oxytocin improves muscle stem cell proliferation *in vivo* after injury

a, Schematic of the experimental procedure. Cardiotoxin (CTX) muscle injury was performed at day 0. Six days before muscle injury and over the course of the experiment, mice were administered OT (1 µg g^{-1} of mice), or vehicle (HBSS) daily. Twelve hours prior to euthanasia, mice were administered with BrdU (50 µg g^{-1} of mice, IP). Three days after muscle injury, tibialis anterior (TA) muscles were isolated.

b, Representative micrographs of 3-day-injured TA muscle cross sections (10 µm) immunostained for BrdU and Desmin and counterstained with DAPI. Right panels represent magnifications of the dashed area from left panels. White arrow indicates a BrdU and Desmin double positive cell, yellow and white arrowheads indicate BrdU or Desmin single positive cells, respectively. Scale bars represent 100 µm (left panels) and 50 µm (right panels).

c, Quantification of the percentage of proliferating myogenic cells (Desmin+ and BrdU+). Data represent mean ± SEM (n=4 YV, n=4 OV, n=4 OOT), one-way ANOVA with post-hoc Newman-Keuls test *: *p* value < 0.05, **: *p* value < 0.01.

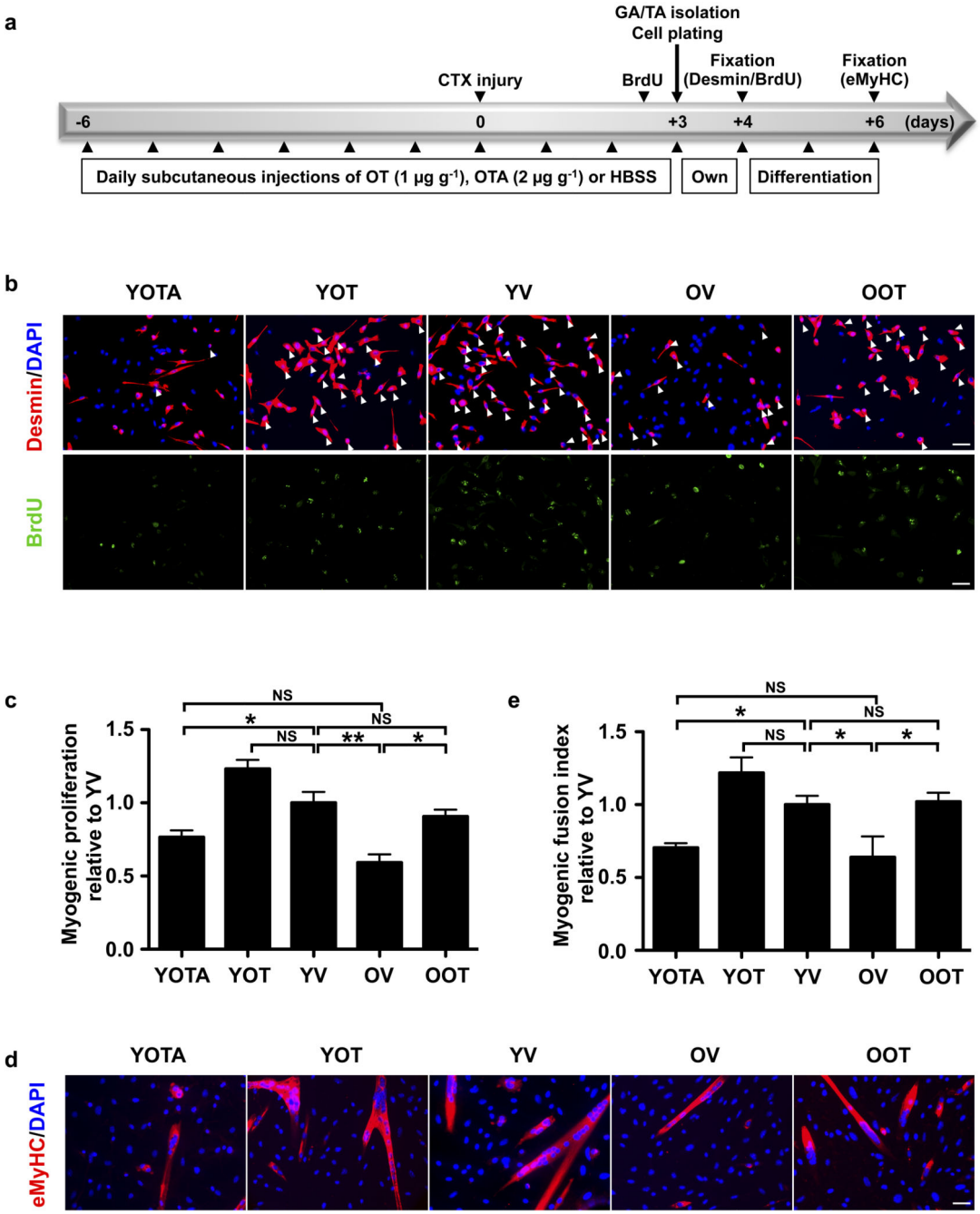

Figure 4. Oxytocin rejuvenates muscle stem cell function in injured tissue

a, Schematic of the experimental procedure. Cardiotoxin (CTX) muscle injury was performed at day 0. Six days before muscle injury and over the course of the experiments, mice were administered OT (1 μg g^{-1} of mice), OTA (2 μg g^{-1} of mice), or vehicle (HBSS) daily. Twelve hours prior to euthanasia, mice were administered with BrdU (50 μg g^{-1} of mice, IP). Three days after muscle injury, GA and TA muscles were isolated and digested into bulk fibers. Cells were cultured in their mouse's respective sera (shortened as "own" on

the schematic) for 24 hours and either fixed and stained for Desmin and BrdU or induced to differentiate for 48 hours and subsequently fixed and stained for eMyHC.

b and **c**, Myogenic cell proliferation. Muscle fiber associated activated satellite cells were isolated 3 days after injury from mice injected with OT, OTA, or vehicle (HBSS), plated in media containing their mouse's respective sera and fixed 24 hours after plating. **b**, Representative micrographs of cells immunostained for Desmin and BrdU and counterstained with DAPI. Scale bars represent 50 μm. **c**, Quantification of the percentage of proliferating myogenic cells (Desmin+ and BrdU+). Data represent mean ± SEM (n=6 YV, n=3 OV, n=3 YOT, n=3 OOT, n=5 YOTA).

d and **e**, Myogenic fusion index. Muscle fiber associated activated satellite cells were isolated 3 days after injury from mice injected with OT, OTA, or vehicle (HBSS), and plated in media containing their mouse's respective sera for 24 hours. Cells were then induced to differentiate in mitogen-low fusion medium for 48 hours, fixed and immunostained for eMyHC using DAPI to label all nuclei. **d**, Representative micrographs. Scale bar represents 50 μm. **e**, Quantification of the percentage of nuclei in eMyHC+ myotubes. Data represent mean ± SEM (n=8 YV, n=5 OV, n=6 YOT, n=6 OOT, n=5 YOTA). In **b-e** YOTA: Young injected with OTA; YOT: Young injected with OT; YV: Young injected with vehicle, OV: Old injected with vehicle; OOT: Old injected with OT. One-way ANOVA with post-hoc Newman-Keuls test *: p value < 0.05, **: p value < 0.01, ***: p value < 0.001, NS: Not Significant.

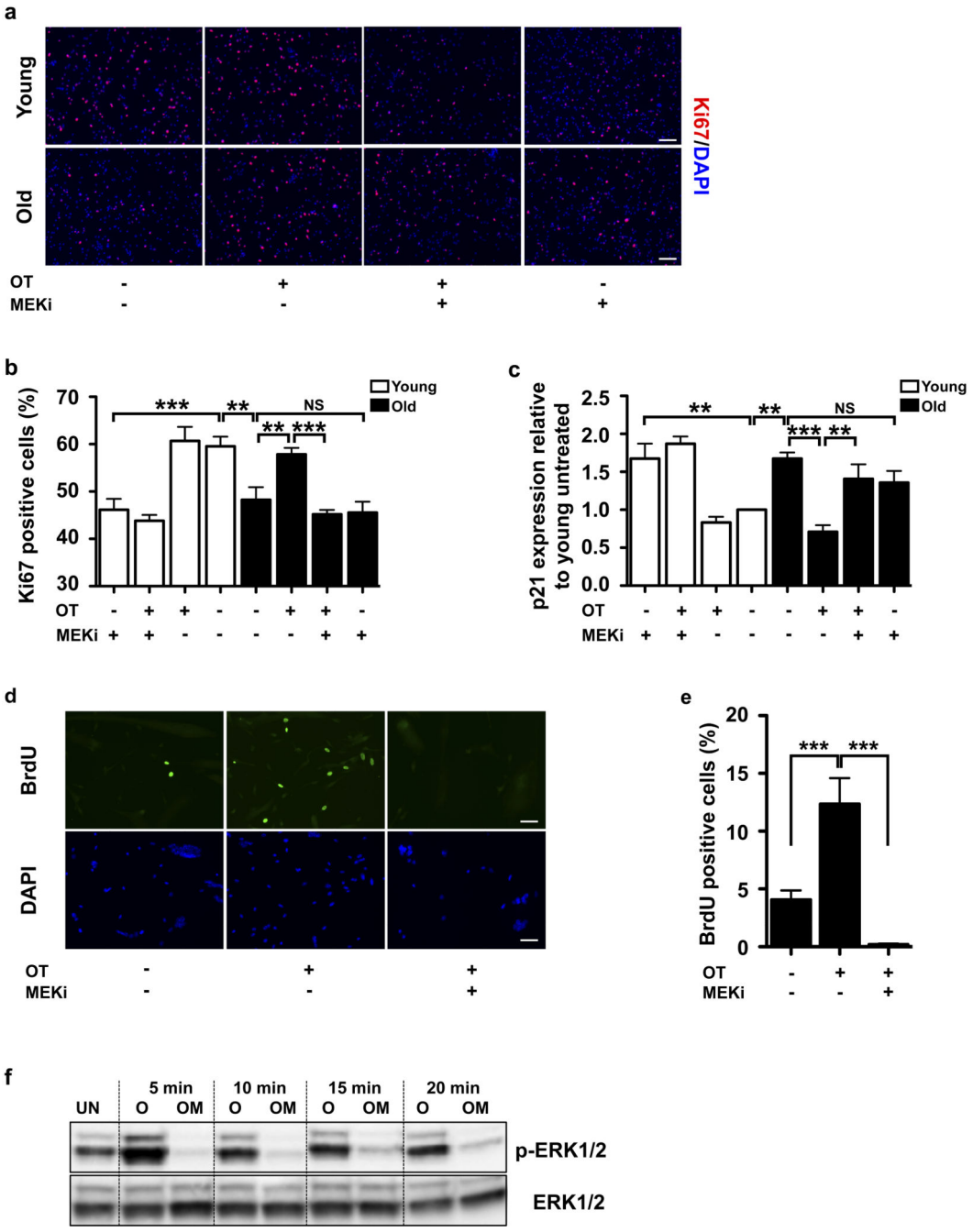

Figure 5. Oxytocin improves myogenic progenitor cell proliferation via activation of the MAPK/ERK pathway

a and b, Activated satellite cells were isolated 3 days after injury from young or old mice, cultured for 24 hours in media containing their own mouse's respective sera supplemented with OT (30 nM), PD98059 MEK inhibitor (50 μM), or OT plus MEK inhibitor, fixed and stained for Ki67 and counterstained for DAPI. **a**, Representative micrographs. Scale bars represent 200 μm. **b**, Quantification of the percentage of proliferating (Ki67+) satellite cells.

Data represent mean ± SEM (n=4 mice per group). Two-way ANOVA with post-hoc Bonferroni test **: *p* value < 0.01, ***: *p* value < 0.001, NS: Not Significant.

c, p21 mRNA relative expression analyzed by qRT-PCR. RNA was extracted from satellite cells isolated and cultured as in **a**. GAPDH was used as reference gene (n=3 mice per group). Two-way ANOVA with post-hoc Bonferroni test **: *p* value < 0.01, ***: *p* value < 0.001, NS: Not Significant.

d and **e**, Primary myogenic progenitors were cultured in the presence or absence of OT (30 nM), and UO126 MEK inhibitor (10 μM) for 48 hours. BrdU was added to the culture medium during the last hour. Cells were then fixed, immunostained for BrdU and counterstained with DAPI. **d**, Representative micrographs. Scale bars represent 50 μm. **e**, The percentages of BrdU positive cells were scored. Data represent mean ± SEM (n= 8 independent experiment performed on different primary cultures). One-way ANOVA with post-hoc Newman-Keuls test ***: *p* value < 0.001, NS: Not Significant.

f, Primary myogenic progenitors were serum starved overnight then treated with OT (30 nM), or OT (30 nM) plus UO126 MEK inhibitor (10 μM) for up to 20 minutes. ERK1/2 and phospho-ERK1/2 were assayed by western blot analysis. O: OT, OM: OT plus UO126 MEK inhibitor.

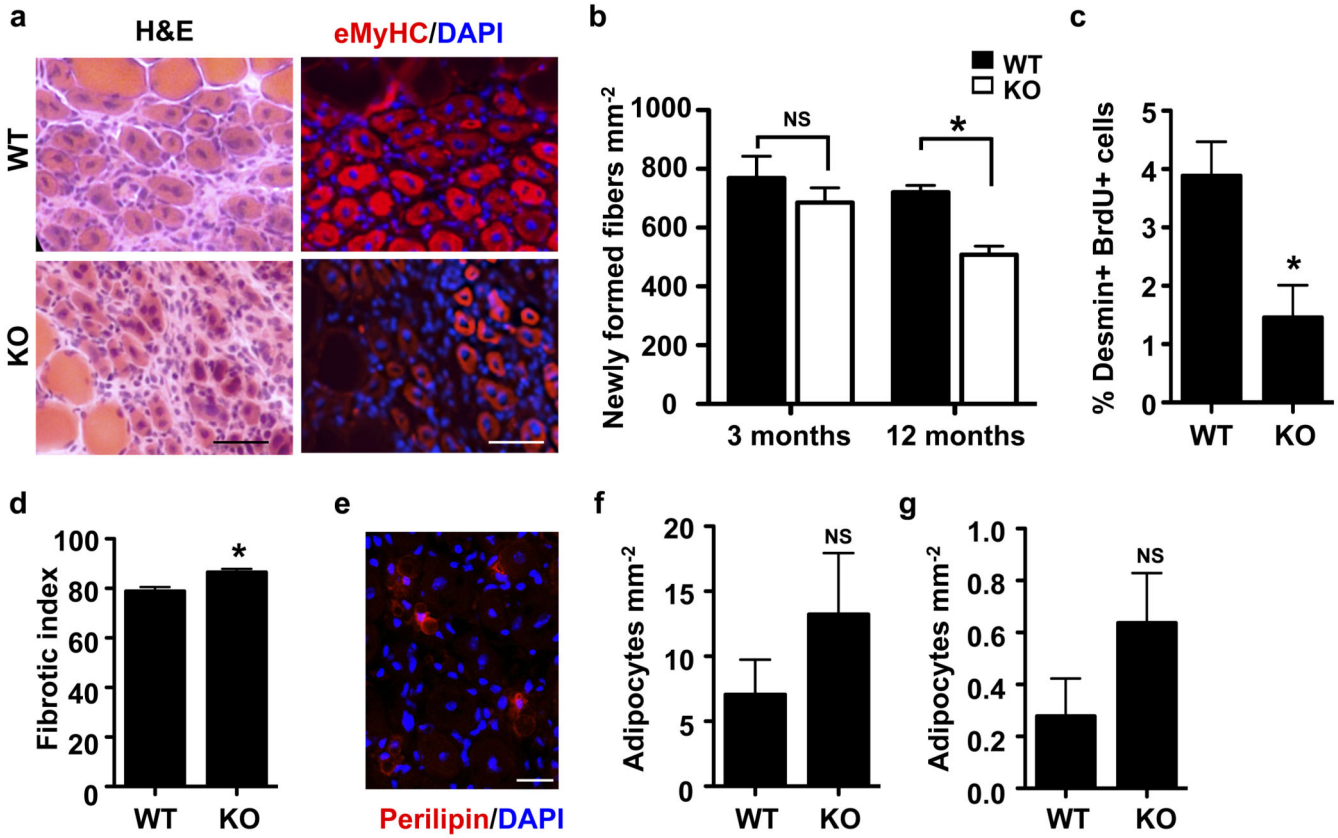

Figure 6. Impaired muscle regeneration in mice lacking oxytocin

a, Hematoxylin and eosin staining (H&E) (top) and eMyHC (bottom) of cardiotoxin-injured gastrocnemius muscle cross sections from 12-month-old wild type (WT) and *Ot* knockout (KO) mice. Scale bars represent 50 μm.

b, Muscle regeneration quantification of 3-month-old and 12-month-old WT or *Ot* KO mice was performed by scoring the number of newly-formed fibers (eMyHC positive fibers with centrally-located nuclei) in the injured area of gastrocnemius cross sections. Data represent mean ± SEM (n=6 WT and n=4 KO for the 3 month old mice, n=4 WT and n=5 KO for the 12 month old). Two-way ANOVA with post-hoc Bonferroni test *: p value < 0.05, NS: Not Significant.

c, Quantification of the percentage of proliferating myogenic cells (Desmin+ and BrdU+) of 3-day-injured TA muscle cross sections immunostained for BrdU and Desmin. Data represent mean ± SEM (n=5 WT, n=5 KO). Two-tailed unpaired Student's t test *: p value < 0.05.

d, Fibrosis quantification of gastrocnemius muscle cross sections 5 days after injury. The fibrotic index represents the percentage of the injury area occupied by connective tissue. Data represent mean ± SEM (n=4 WT and n=4 KO). Two-tailed unpaired Student's t test *: p value < 0.05.

e, Representative micrograph of perilipin immunostaining on 5-day-cardiotoxin-injured gastrocnemius muscle cross section. Scale bar represents 50 μm.

f and **g**, Adipocyte numbers (perilipin positive cells) per injured (**f**) or un-injured (**g**) area from WT and *Ot* KO mice. Data represent mean ± SEM (n=3 WT and n=5 KO). Two-tailed unpaired Student's t test, NS: Not Significant.

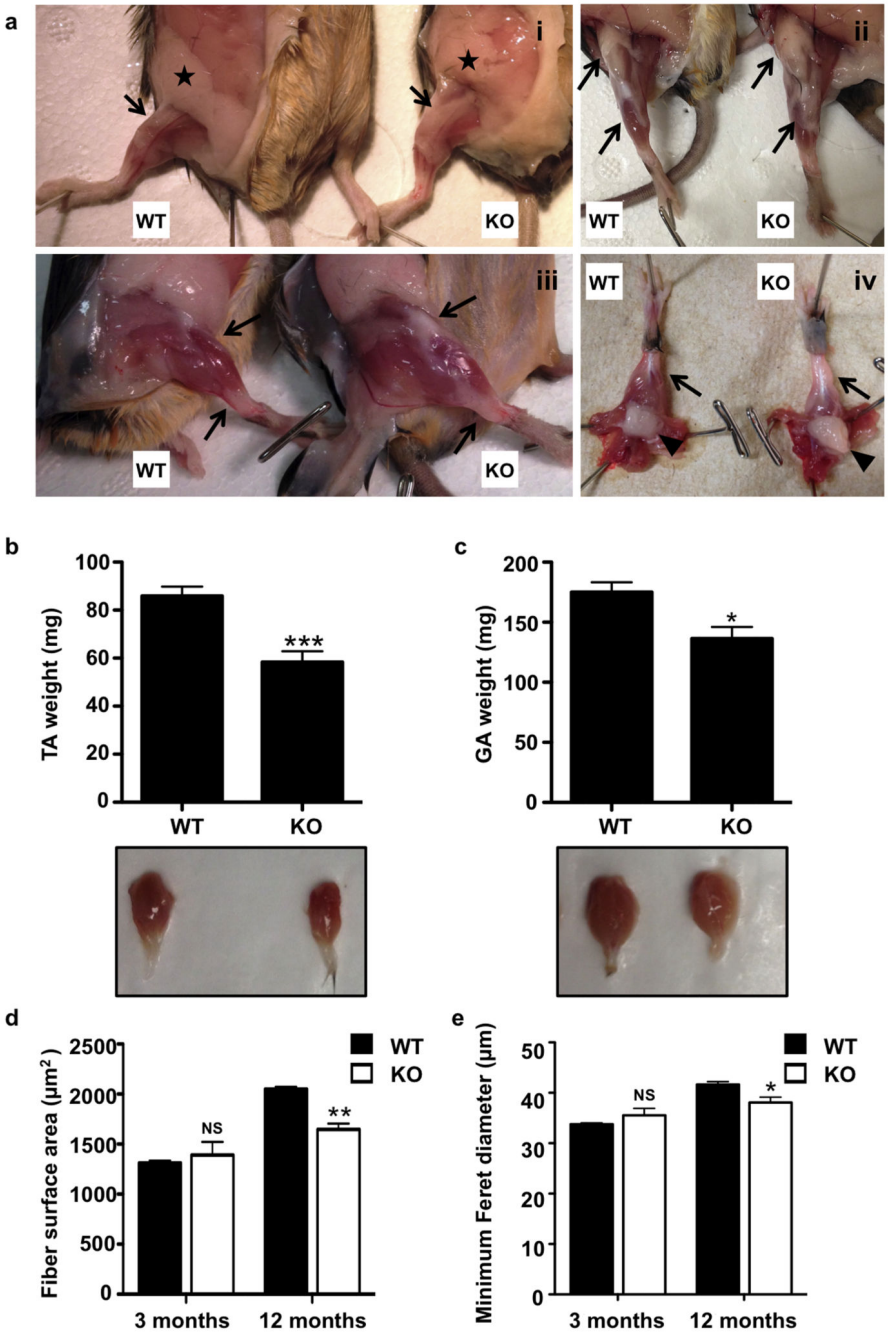

Figure 7. Mice lacking oxytocin develop premature sarcopenia

a, Representative photographs of *Ot* KO and WT mice hind limb skeletal muscles (right leg) after the skin was carefully removed (WT and KO mice are presented side by side on each photograph). Visualization of perimuscular adipose tissue deposition (arrows) and of exposed intermuscular adipose tissue (arrowheads). (i) Ventral view, arrows indicate the adipose tissue on the internal part of the quadriceps. The star shows that *Ot* KO mice display increased posterior subcutaneous adipose tissue. (ii) Ventral view showing adipose tissue deposition over the quadriceps (top arrows) and the tibialis anterior (bottom arrows). (iii)

Lateral view showing adipose tissue deposition covering the quadriceps (top arrows) and the tibialis anterior and gastrocnemius (bottom arrows). (iv) Dorsal view showing the intermuscular adipose tissue deposition of the hind leg (arrowheads) and the adipose tissue covering the gastrocnemius muscle (arrows). As compared to the WT littermates, the KO mice have an increase in fat tissue in all the studied muscle groups, and visibly reduced muscle, which is studied in more detail and quantified below.

b, TA and **c**, GA muscles from 12-month-old WT or *Ot* KO mice were weighed. Data represent mean ± SEM (top), representative pictures (bottom). Two-tailed unpaired Student's t test *: p value < 0.05, ***: p value < 0.001, n=5 WT and n=10 KO mice.

d, The surface area and **e**, The minimum Feret's diameter were measured using WT and *Ot* KO muscle cross section stained with Hematoxylin and eosin. Data represent mean ± SEM (n=4 mice per group), two-way ANOVA with post-hoc Bonferroni test *: p value < 0.05, **: p value < 0.01, NS: Not Significant.